[redacted]

[illegible]

Classification cancelled (or changed to) Unclassified

Per Tech Pub Announcement #109

29 Nov 56

By ...

GRADE OF OFFICER MAKING CHANGE)

DATE

NATIONAL ADVISORY COMMITTEE FOR AERONAUTICS

RESEARCH MEMORANDUM

FLIGHT INVESTIGATION OF THE ROLLING EFFECTIVENESS OF FINGERED SEMAPHORE SPOILERS ON A TAPERED 45° SWEPTBACK WING BETWEEN MACH NUMBERS 0.6 AND 1.3

By James D. Church

SUMMARY

A free-flight investigation of a fingered semaphore spoiler and an equivalent solid spoiler configuration has been conducted to determine some effects of spoiler projection, porosity, and chordwise position on the rolling effectiveness and drag of the spoiler arrangements through the range of Mach number from 0.6 to 1.3. The wings were swept back 45° along the quarter-chord line, had an aspect ratio of 3.56, a taper ratio of 0.30, and NACA 64A007 airfoil sections parallel to the free stream. Both the solid and fingered spoiler systems tested extended from 30 to 70 percent of the wing semispan and were located along a line of constant wing thickness. Test results indicated that the fingered semaphore spoilers had less rolling effectiveness and drag than the solid spoiler configuration. Variation of the rolling effectiveness and drag of the fingered semaphore spoilers with projection was nearly linear at subsonic and supersonic speeds for spoiler deflections up to approximately 45°. At these speeds, deflections larger than 45° resulted in little change in effectiveness.

INTRODUCTION

Past studies of effectiveness, hinge moment, and aeroelastic effects of spoilers indicate the possible use of this device as a low-force lateral control for high-speed aircraft. (See refs. 1 to 7.) In addition, these data show that spoiler porosity and sweepback can be utilized to reduce the time lag, yaw magnitude, and loss in effectiveness with angle-of-attack characteristics of spoiler controls. Unpublished preliminary flight tests also indicate that spoiler porosity advantageously affects the linearity of spoiler hinge moments. The rolling effectiveness and

drag of a fingered semaphore spoiler configuration evolved from these studies has been investigated through the use of rocket-powered models by the Langley Pilotless Aircraft Research Division.

Some effects of spoiler projection, porosity, and chordwise position on rolling effectiveness and drag of this spoiler configuration were obtained by experiment or comparison for a range of Mach number from 0.6 to 1.3. Damping in roll was determined for the tapered sweptback wing having an NACA 64A007 airfoil section used in these tests. In addition, some of the effects of roll helix angle on spoiler rolling-moment coefficient were found.

These results are presented herein and are compared with linear theory and other rocket-model data.

SYMBOLS

b	diameter of circle generated by wing tips, 2.56 ft
b_s	span of basic spoiler slot, $0.400b/2$
y	spanwise distance, measured from and normal to model center line, ft
c	local wing chord measured parallel to model center line, ft
c_e	wing chord at midspan of basic spoiler slot, 0.720 ft
$\bar{c}$	wing mean aerodynamic chord, 0.789 ft
s	total frontal area of spoilers on one wing semispan above wing surface, measured perpendicular to free stream, sq ft
h	maximum spoiler height above wing, measured normal to wing chord plane, ft
h/c_e	spoiler height in percent chord
δ	spoiler deflection, measured in plane of spoilers and normal to wing chord plane (spoiler on upper surface when wing on right side looking forward), deg
S	area of three wings measured to model center line, 2.77 sq ft
A	wing aspect ratio, $3b^2/2S = 3.56$

λ wing taper ratio (ratio of tip chord to chord at model center line), 0.30

i_ω average incidence of three wings, measured in plane normal to wing chord plane and parallel to free stream, deg

m concentrated couple, applied near wing tip in plane parallel to free stream and normal to wing chord plane, ft-lb

θ angle of twist produced by m at any station along wing span, measured parallel to plane of m, radians

θ/m wing torsional flexibility parameter, radians/ft-lb

I_x moment of inertia about longitudinal axis, slug-ft^2

T nonaerodynamic torque, lb-ft

M Mach number

q dynamic pressure, lb/sq ft

V free-stream velocity, ft/sec

R Reynolds number based on wing mean aerodynamic chord

p rolling velocity, radians/sec

$\dot{p}$ rolling acceleration, dp/dt, radians/sec^2

pb/2V wing-tip helix angle, radians

C_D drag coefficient, $\frac{\text{Drag}}{qS}$

ΔC_D incremental drag coefficient of three spoilers (one per wing)

C_l rolling-moment coefficient, $\frac{\text{Rolling moment}}{qbS}$

C_{l_p} damping-in-roll derivative of wing-body combination per radian, $(\delta = 0^\circ) \approx \frac{\Delta C_l}{\Delta pb/2V}$

C_{l_s} spoiler rolling-moment coefficient,

$$\frac{\text{Total rolling moment produced by all spoilers}}{qSb}$$

[redacted]

Subscripts:

0	out-of-trim component
1	sustainer-on flight
2	coasting flight

MODELS AND TESTS

The models used in this investigation, with the exception of wing design and addition of spoilers, were identical with the three-winged vehicles of references 8 and 9. Each body consisted of a cylindrical wooden fuselage with a spinsonde nose section and an internal sustainer rocket motor with four canted nozzles to produce torque. The solid aluminum-alloy wings were swept back 45.1° along the quarter-chord line, had an aspect ratio of 3.56, a taper ratio of 0.30, NACA 64A007 airfoil sections parallel to the free stream, and a spoiler location along a line of constant wing thickness. Figure 1 gives the geometric details of the wing-body combination and the spanwise and chordwise positions of the basic spoiler slot. Illustrations of a typical test vehicle prior to launching are shown in figure 2.

The spoilers tested in this investigation were formed from aluminum-alloy blanks machined to represent fingered semaphore-type spoilers with deflections of 20°, 45°, 65°, and 90°. One model's wings were slotted to duplicate the gap configuration that would result from an application of the tested spoiler arrangement to a full-scale movable spoiler system at a deflection of 90°. In addition, a solid spoiler model was constructed. Sketches of some of the spoiler types are presented in figure 3, and photographs of two of the wing-spoiler combinations are shown in figure 4. Details of an individual fingered spoiler are illustrated in figure 5. For the purpose of comparing the fingered semaphore spoiler with the solid spoiler, spoiler deflection was resolved into the maximum spoiler height and the total frontal area shown in figure 6.

Average values of the wing torsional flexibility are plotted in figure 7 as the variation of the parameter θ/m with wing span.

A booster-rocket system propelled the models to a Mach number of about 0.6 at which point the model-booster combinations separated; the sustainer motors then accelerated the models to a Mach number of approximately 1.4. During the sustainer-on and coasting portions of the flights, a CW Doppler radar set measured the vehicle's flight-path velocities and accelerations, and a tracking radar set determined the model's position in space. Rolling-velocity and acceleration measurements were obtained

by means of special radio equipment. Atmospheric data over the required altitude range were measured by radiosondes.

Typical variations of Reynolds number and dynamic pressure with Mach number for both the sustainer-on and coasting portions of the flights of all models are presented in figure 8. The maximum deviation from the mean value of Reynolds number at any given Mach number was of the order of $\pm 6 \times 10^5$, whereas the corresponding deviation for the dynamic pressure was about ± 150 lb/sq ft.

REDUCTION OF DATA AND ACCURACY

The technique presented herein is basically an extension of the method used in reference 8, where a known nonaerodynamic forcing moment producing roll was used with measurements of model inertia, Mach number, and rolling velocity to yield the damping-in-roll derivative C_{l_p} by equating the moments acting on the model in sustainer-on and coasting flight.

In the present tests, the data obtained from each model's flight were reduced to drag coefficient and rolling effectiveness $pb/2V$ in the manner of reference 10. The $pb/2V$ values so obtained were corrected for the effects of wing incidence i_ω resulting from construction tolerances by the method outlined in reference 11. Rolling-moment coefficients due to the three spoilers of each model C_{l_s} were obtained by using these corrected $pb/2V$ values in conjunction with the measured C_{l_p} data from the slotted wing configuration in the following manner: the single degree of freedom-in-roll equation for sustainer-on flight, where the out-of-trim component C_{l_0} is assumed negligible because of the i_ω correction just mentioned, yields

$$I_{x_1}\dot{p}_1 - C_{l_p}\frac{p_1 b}{2V_1} q_1 bS = T + C_{l_{s_1}} q_1 bS \tag{1}$$

Solving equation (1) for $C_{l_{s_1}}$ gives

$$C_{l_{s_1}} = \frac{I_{x_1}\dot{p}_1 - T}{q_1 bS} - C_{l_p}\frac{p_1 b}{2V_1} \tag{2}$$

and, similarly, C_{l_s} for coasting flight becomes

$$C_{l_{s_2}} = \frac{I_{x_2}\dot{p}_2}{q_2 bS} - C_{l_p}\frac{p_2 b}{2V_2} \tag{3}$$

The reliability of this method of obtaining spoiler rolling-moment coefficients is based on the assumptions that spoiler projection in no way affects C_{l_p} and that C_l varies linearly with p. Possible adverse effects of the former assumption are dealt with in the section entitled "Results and Discussion," and effects of the latter assumption are adequately covered in reference 8. Figure 9 presents typical variations of the parameters used in the solution of equations (2) and (3) over the range of Mach number investigated.

The C_{l_p} values obtained for the slotted wing configuration that were used in the preceding equations for determining spoiler rolling-moment coefficients were determined by using the equation

$$\frac{\Delta C_l}{\Delta pb/2V} = \frac{\left(\frac{I_{x_1}\dot{p}_1}{q_1} - \frac{I_{x_2}\dot{p}_2}{q_2}\right) - \frac{T}{q_1}}{bS\left(\frac{p_1 b}{2V_1} - \frac{p_2 b}{2V_2}\right)} \tag{4}$$

A detailed description of this method of evaluating C_{l_p} can be found in reference 8.

Although the accuracy of the values of C_{l_s} calculated by using equations (2) and (3) depends on the out-of-trim corrections for pb/2V described previously, the value of C_{l_p} determined by equation (4) is independent of this factor if the assumption is made that C_{l_0} is constant with variations in pb/2V at a given Mach number.

The accuracy of the test parameters and the components necessary to their determination is estimated from previous experience and mathematical analysis to be within the following limits:

Variable	Subsonic	Supersonic
T/q, cu ft	±0.003	±0.001
M	±.010	±.005
pb/2V, radians . . .	±.003	±.002
C_D	±.003	±.002
C_{l_p}	±.020	±.010
C_{l_s}	±.0010	±.0008

Although these estimations apply to the absolute value of the quantities, in computations involving sensitivity (rate of change of a variable with Mach number) possible errors can be considered to be roughly one-half as large as those shown. References 8 and 10 give a more complete analysis of the origin of sources of error in the determination of the test variables. The probable errors in the measurements of i_w and h/c are ±0.05° and ±0.0005, respectively.

No aeroelasticity corrections have been applied to the presented results since reference 7 indicates that wings having torsional stiffnesses of the order shown in figure 7 are not subject to large aeroelastic effects because of spoilers.

RESULTS AND DISCUSSION

Rolling Effectiveness

The results from the coasting flights of this investigation are presented in the form of variations of pb/2V and C_D with Mach number in figure 10. Before discussing the figure, two flight irregularities must be mentioned: namely, reliable drag data for model 5 were not obtained, and no data were obtained for most of the second model's ($\delta = 20°$) coasting flight because of a structural failure shortly after sustainer burnout. The latter occurrence necessitated the use of sustainer-on data for this flight as a qualitative measure of effectiveness for the low spoiler projections. The values of pb/2V shown in figure 10 for this model were computed using $C_{l_{s_1}}$ obtained from equation (2) for sustainer-on flight to yield the steady-state roll with the torque term removed.

Apparent from figure 10 is the large transonic reduction in effectiveness encountered by all spoilers except the 20° fingered condition. Although the solid spoiler maintained a substantial margin of effectiveness over the fingered configurations in the subsonic region, it had a larger percentage reduction at transonic and supersonic speeds. Also evident from figure 10 is the relatively small change in effectiveness for fingered spoiler deflections much larger than 45°.

An effect of spoiler chordwise position can be gained from figure 11 where the data for model 6 are compared with the results of reference 7. These reference data were obtained for a solid spoiler configuration similar to that of the present test but located along the 0.7c position as opposed to the location shown in figure 1 by using a method described in the subject report which utilizes plots of $pb/2V$ against spoiler spanwise location at various Mach numbers. Although the wing of the reference tests was slightly different from that used for this investigation ($A = 4.00$; $\lambda = 0.60$; NACA 65A006 airfoil section), it is felt that these data primarily reflect the difference in spoiler chordwise location.

The solid spoiler of the present test had a variation of effectiveness with Mach number that was less than that of reference 7 except between Mach numbers 0.76 and 0.92; this result is consistent with past experience of the effect of forward chordwise movement of spoilers. Although a direct correlation of the two investigations with regard to magnitude would be of dubious value because of the manner in which the data of reference 7 were used, the data indicate that forward chordwise movement of the spoiler, in general, resulted in less effectiveness.

Figure 12 has been prepared to illustrate better the useful range of spoiler deflections with regard to linearity for the fingered semaphore-type spoiler arrangement. With the exception of $M = 1.0$, spoiler deflections up to values approaching 45° yielded near linear changes in effectiveness over the speed range tested. Larger deflections exhibited a pronounced loss in effectiveness per unit spoiler deflection over the entire Mach number range. It should be noted that the possibility of reversal in effectiveness for the low spoiler projections was not investigated; however, the shape of the curves indicates that this phenomenon would be restricted to spoiler deflections much less than 20° and to the transonic speed region.

The reduction in $pb/2V$ from the solid to the fingered spoiler system is more apparent in figure 12 than in figure 10. For example, at a spoiler deflection of 26.5°, where the maximum heights of the fingered and solid spoilers are equal, the loss in $pb/2V$ due to porosity was approximately 61 percent at subsonic and 64 percent at supersonic speeds for a corresponding frontal-area reduction of 69 percent. Noteworthy is the possibility of decreasing this loss by increasing the number of fingered spoilers per basic wing slot. Unpublished wind-tunnel data indicate

that increasing the number of spoiler paddles from 6 to 11 by the introduction of another row of spoilers in the existing spaces between the original paddles (this system is referred to as double-row spoilers) raises the level of effectiveness to values approaching that of the solid configuration.

Drag

A drag comparison of data from reference 9 with the slotted wing configuration of the present test (see fig. 10) shows the maximum increase in drag coefficient due to the wing gaps that would result from an application of the tested spoiler arrangement to a full-scale movable spoiler system to be about 0.003. Inasmuch as the effects of spoiler chordwise location, porosity, and projection are more readily apparent when incremental drag coefficient is employed, figures 11 and 13 are presented. Since the thickness corrections to the data of reference 9 are at best only approximations, the results of model 1 were used to reduce the data of figure 10 to ΔC_D.

The drag data of reference 7 shown in figure 11 were obtained in a manner similar to that described for $pb/2V$. Again the interpolated data of reference 7 are not of sufficient accuracy to justify comment on the relative magnitude of the two investigations beyond the obvious remark that a comparison of the solid spoiler of the present test with that of reference 7 shows that forward chordwise movement of the spoiler resulted in consistently higher values of ΔC_D.

For the six Mach numbers shown in figure 13 a decrease of approximately 50 to 60 percent in the drag due to spoiler deflection occurred from the solid to the fingered spoiler system at the correlation deflection of 26.5°. With regard to the linearity of ΔC_D, it is apparent that the fingered spoilers had a more nearly linear variation of ΔC_D than $pb/2V$ with spoiler deflection for the same deflection range at the six Mach numbers shown.

Wing Damping in Roll

The application of equation (4) to the results from the slotted-wing model yielded the curve for C_{l_p} shown in figure 14. A comparison of this curve with the curve for C_{l_p} from reference 9 for a plain wing of similar plan form indicates that the wing gaps of the test configuration have little or no effect on C_{l_p}. The correlation of subsonic theory corrected for compressibility (ref. 12) with the present test appears very good insofar as predicting the variation with Mach number of the

parameter; however, a constant overestimate of about 0.06 exists. As could be anticipated, the supersonic uniplanar linearized theory (ref. 13) yields a poor estimate of C_{l_p} for the type of plan form tested for reasons such as the speed region, three-fin arrangement employed, wing flexibility, wing-body interference, and other considerations.

Rolling-Moment Coefficient

The results of equations (2) and (3) for eight Mach numbers are shown in figure 15. The apparent scatter at any one spoiler deflection represents incremental differences in spoiler effectiveness due to an increase in $pb/2V$ from coasting to sustainer-on flight caused by the torque nozzles; increases in $pb/2V$ are such as to increase the roll helix angle in a direction that blankets the flow over the spoilers. Important is the negligible change in C_{l_s} caused by changes in $pb/2V$ of the order of 0.02 to 0.07 radian for all spoilers at all Mach numbers shown except 0.95 and 1.0. This fact shows that little error should result from using the calculated values of $pb/2V$ for model 2 in the section on "Rolling Effectiveness." (See figs. 10 and 12.) Although the relatively large change in C_{l_s} due to $pb/2V$ at transonic speeds tends to reduce the loss in effectiveness in this speed region, the ability of the spoilers to produce roll at various rolling velocities is greatly obscured because the effects on effectiveness, time lag, and wing-dropping caused by the spoilers are inseparable by virtue of the technique utilized to obtain C_{l_s}.

The validity of the preceding results is dependent on the assumption of an invariant value of C_{l_p} with the addition of spoilers. If the spoilers produce an effect similar to an addition in wing thickness, reference 14 shows that in the transonic region some wing-dropping may result. Thus, the effect of spoilers on C_{l_p} should be approximately constant at all speeds with possibly a small bump near $M = 1.0$. Although the foregoing result is not rigorous, the magnitude of any change in C_{l_p} due to the spoilers would have to be very large to invalidate the trends shown in figure 15.

The loss in effectiveness due to porosity is strikingly obvious in figure 15; for example, this loss is approximately 64 percent at subsonic speeds and 67 percent at supersonic speeds at the correlation deflection of 26.5°. Thus, the evaluation of C_{l_s} shows the loss in effectiveness to be more nearly a direct function of the area reduction than for the $pb/2V$ comparison. The C_{l_s} variation with deflection for the fingered

spoilers is approximately linear for deflections from 0° to 45°, becoming nonlinear above this deflection range as was the case for $pb/2V$. (See fig. 12.) In the interest of maintaining the sense of the C_{l_s} change with $pb/2V$ and of regaining the effectiveness lost by both porosity and forward chordwise position, the use of fingered semaphore spoilers in a double row (such as to produce a solid saw-toothed area) nearer the 0.7 chord that was previously mentioned is suggested.

CONCLUSIONS

A rocket-model investigation has been made of both a fingered semaphore and a solid spoiler system mounted along a line of constant wing thickness. The test wings were swept back 45° along the quarter-chord line, had an aspect ratio of 3.56, a taper ratio of 0.30, and NACA 64A007 airfoil sections parallel to the free stream. The following conclusions are presented:

1. The fingered semaphore spoiler had less rolling effectiveness and drag than the solid spoiler configuration.

2. Variation of the rolling effectiveness for the fingered semaphore spoiler with spoiler projection was linear for deflections up to approximately 45° at subsonic and supersonic speeds. At these speeds, deflections larger than 45° resulted in little change in effectiveness.

3. Fingered, semaphore spoiler drag varied linearly with spoiler deflection over the deflection range from 0° to about 45° for the speed range tested.

4. All spoiler rolling-moment coefficients were apparently unaffected by roll-helix-angle variations except at transonic speeds.

5. Comparison of the present results with other rocket-model data (for a similar configuration) indicated that forward chordwise movement of the spoiler along the wing chord decreased the rolling effectiveness and increased the drag of the solid spoiler configuration.

Langley Aeronautical Laboratory,
National Advisory Committee for Aeronautics,
Langley Field, Va., November 6, 1953.

REFERENCES

1. Kramer, May, Zobel, Theodor W., and Esche, C. G.: Lateral Control by Spoilers at the DVL. NACA TM 1307, 1951.

2. Bollech, Thomas V., and Pratt, George L.: Effects of Plain and Step Spoiler Location and Projection on the Lateral Control Characteristics of a Plain and Flapped 42° Sweptback Wing at a Reynolds Number of 6.8×10^6. NACA RM L9L20a, 1950.

3. Vogler, Raymond D.: Wind-Tunnel Investigation at High Subsonic Speeds of Spoilers of Large Projection on an NACA 65A006 Wing With Quarter-Chord Line Swept Back 32.6°. NACA RM L51L10, 1952.

4. Fikes, Joseph E.: Hinge-Moment and Other Aerodynamic Characteristics at Transonic Speeds of a Quarter-Span Spoiler on a Tapered 45° Sweptback Wing of Aspect Ratio 3. NACA RM L52A03, 1952.

5. Strass, H. Kurt: Summary of Some Effective Aerodynamic Twisting-Moment Coefficients of Various Wing-Control Configurations at Mach Numbers From 0.6 to 1.7 As Determined From Rocket-Powered Models. NACA RM L51K20, 1952.

6. Strass, H. Kurt, and Marley, Edward T.: Rocket-Model Investigation of the Rolling Effectiveness of a Fighter-Type Wing-Control Configuration at Mach Numbers From 0.6 to 1.5. NACA RM L51I28, 1951.

7. Schult, Eugene D., and Fields, E. M.: Free-Flight Measurements of Some Effects of Spoiler Span and Projection and Wing Flexibility on Rolling Effectiveness and Drag of Plain Spoilers on a Tapered Sweptback Wing at Mach Numbers Between 0.6 and 1.6. NACA RM L52H06a, 1952.

8. Edmondson, James L., and Sanders, E. Claude, Jr.: A Free-Flight Technique for Measuring Damping in Roll by Use of Rocket-Powered Models and Some Initial Results for Rectangular Wings. NACA RM L9I01, 1949.

9. Sanders, E. Claude, Jr.: Damping in Roll of Straight and 45° Swept Wings of Various Taper Ratios Determined at High Subsonic, Transonic, and Supersonic Speeds With Rocket-Powered Models. NACA RM L51H14, 1951.

10. Sandahl, Carl A., and Marino, Alfred A.: Free-Flight Investigation of Control Effectiveness of Full-Span 0.2-Chord Plain Ailerons at High Subsonic, Transonic, and Supersonic Speeds To Determine Some Effects of Section Thickness and Wing Sweepback. NACA RM L7D02, 1947.

11. Strass, H. Kurt, and Marley, Edward T.: Rolling Effectiveness of All-Movable Wings at Small Angles of Incidence at Mach Numbers From 0.6 to 1.6. NACA RM L51H03, 1951.

12. Polhamus, Edward C.: A Simple Method of Estimating the Subsonic Lift and Damping in Roll of Sweptback Wings. NACA TN 1862, 1949.

13. Malvestuto, Frank S., Jr., Margolis, Kenneth, and Ribner, Herbert S.: Theoretical Lift and Damping in Roll at Supersonic Speeds of Thin Sweptback Tapered Wings With Streamwise Tips, Subsonic Leading Edges, and Supersonic Trailing Edges. NACA Rep. 970, 1950. (Supersedes NACA TN 1860.)

14. Stone, David G.: Wing-Dropping Characteristics of Some Straight and Swept Wings at Transonic Speeds As Determined With Rocket-Powered Models. NACA RM L50C01, 1950.

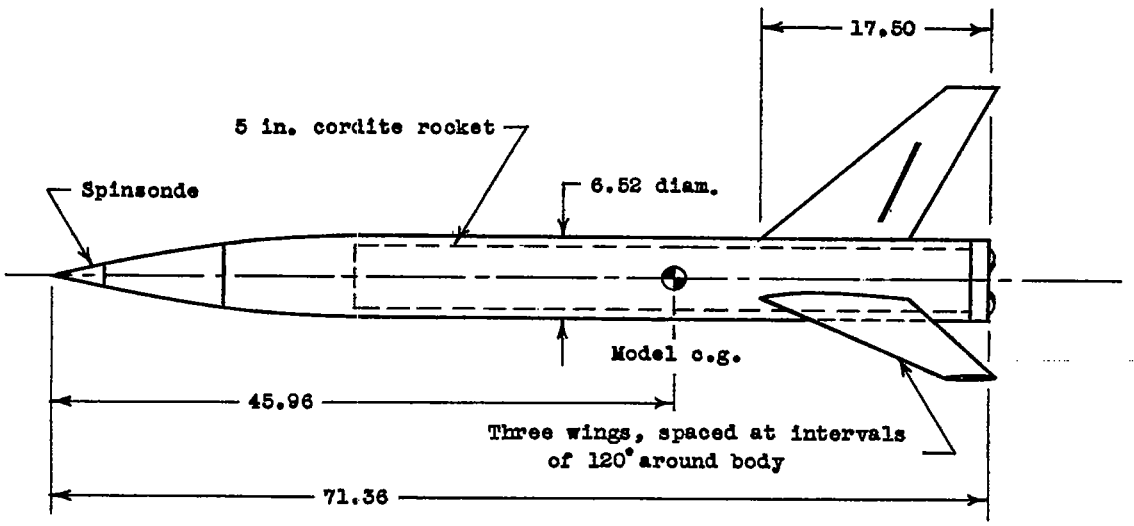

Model plan view

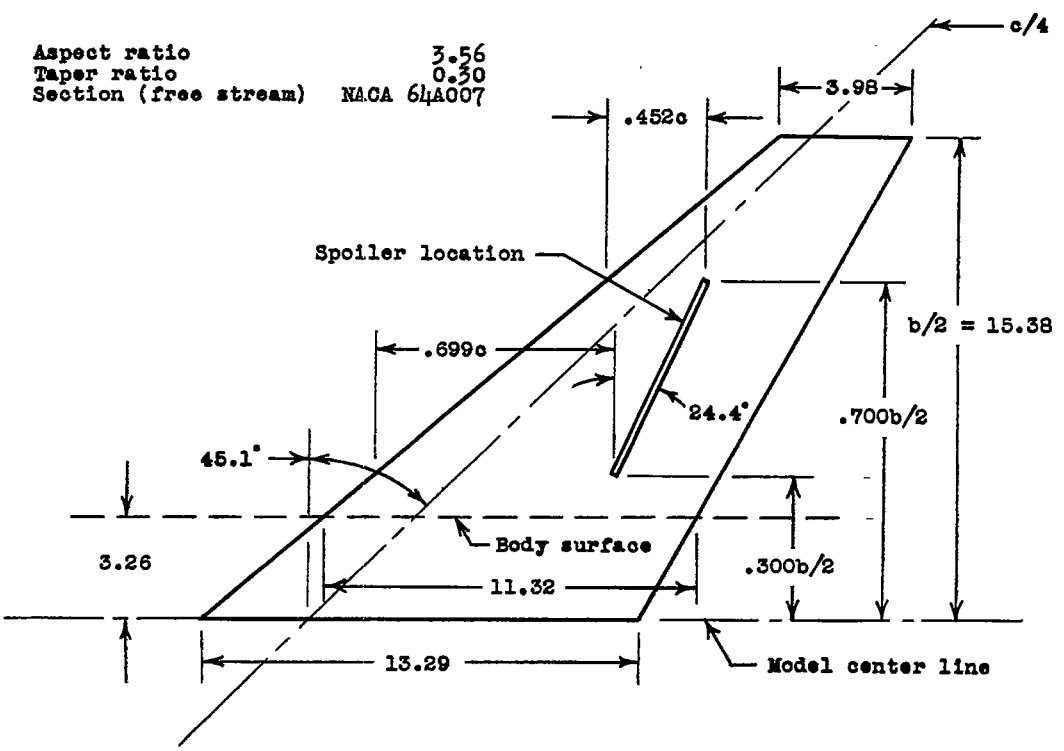

Wing plan form and location of basic spoiler slot

Figure 1.- Geometric details of test vehicle. All dimensions are in inches unless otherwise noted.

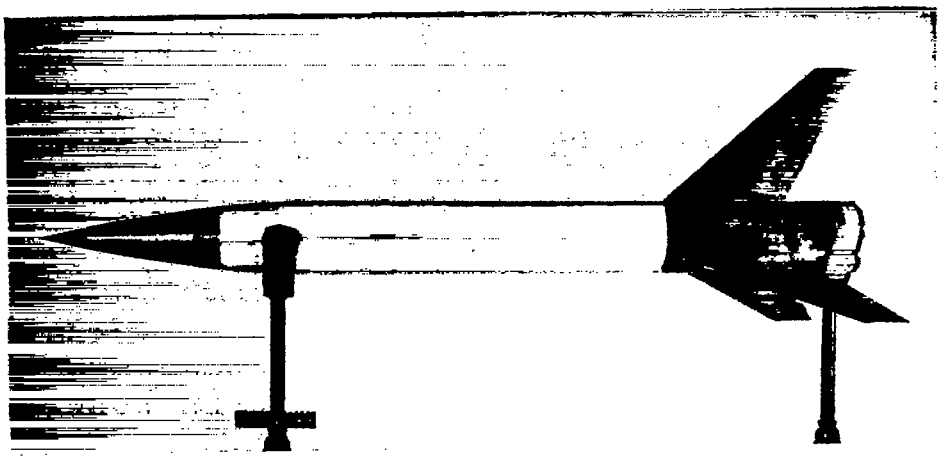

L-76012.1

(a) Model plan view.

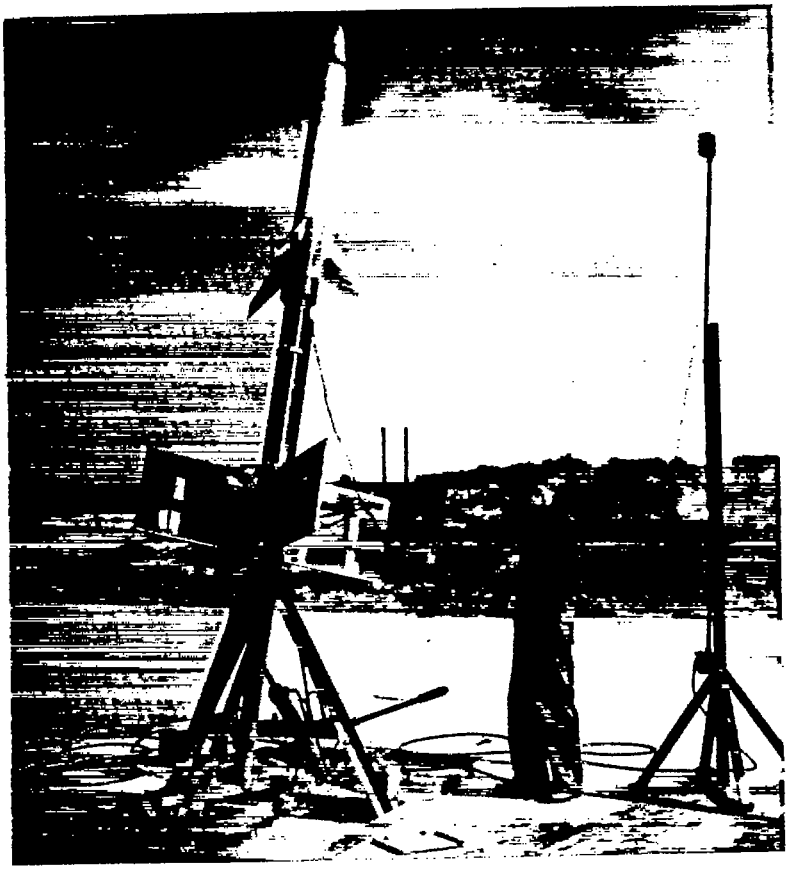

L-77516.1

(b) Preparatory to launching.

Figure 2.- Typical test vehicle.

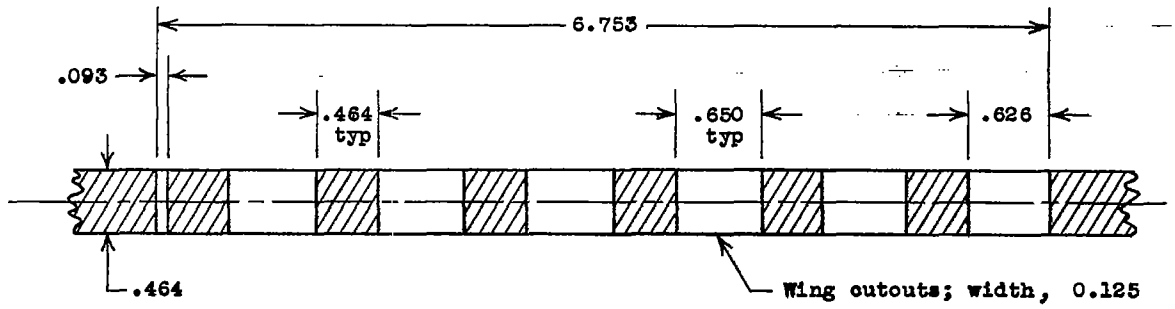

Slotted-wing configuration

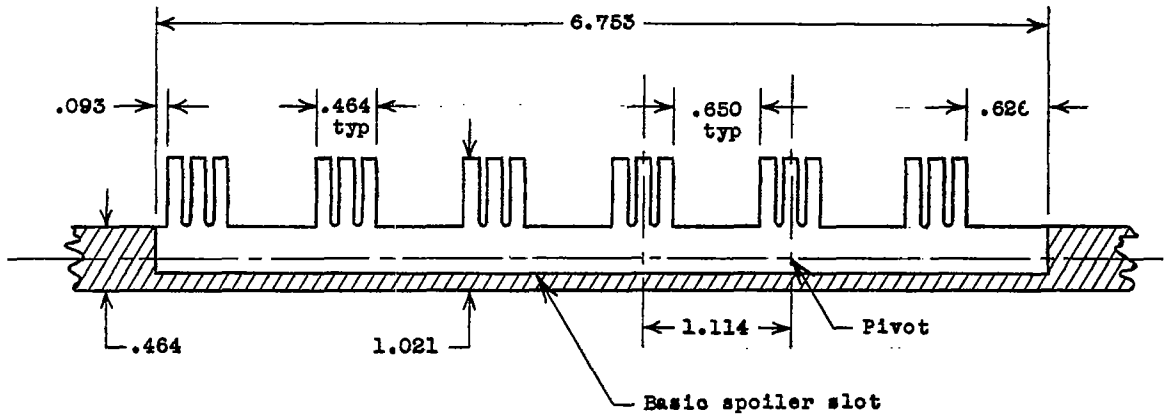

Maximum spoiler projection

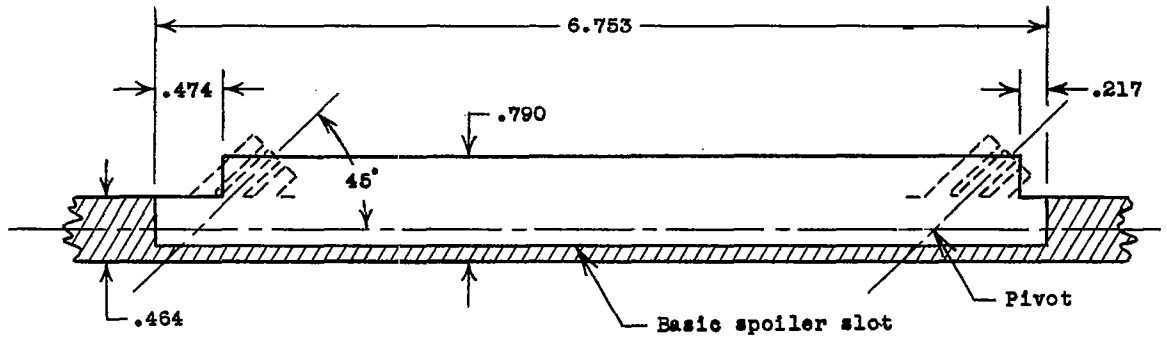

Solid spoiler with 45° rotation configuration for comparison

Figure 3.- Sections as one looks forward in plane of basic spoiler slot. All dimensions are in inches.

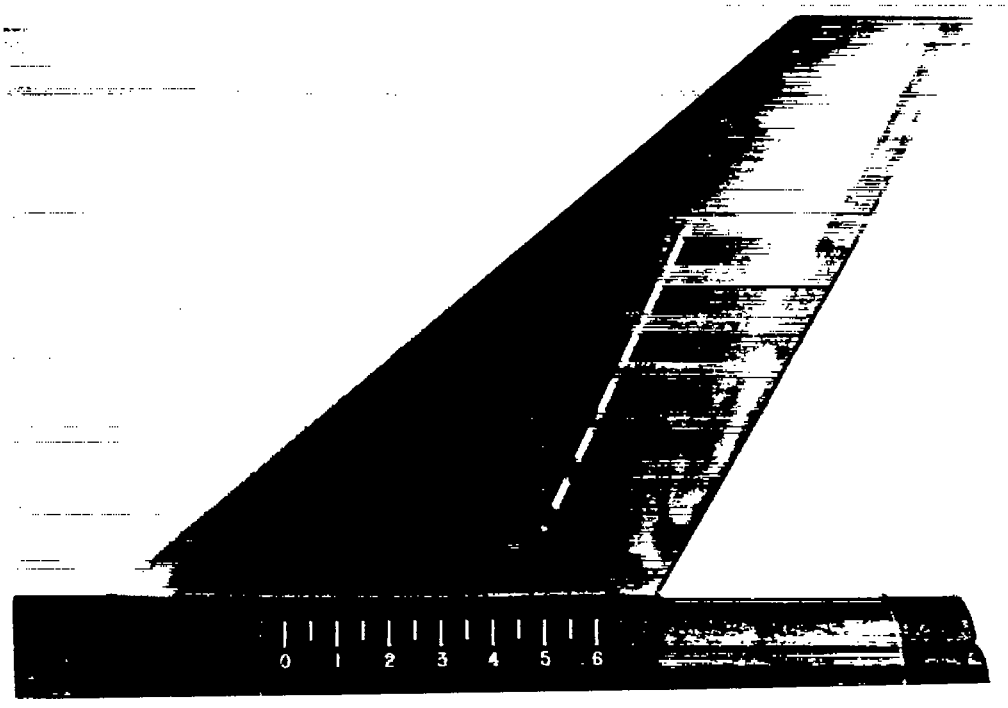

L-76258

(a) Slotted wing.

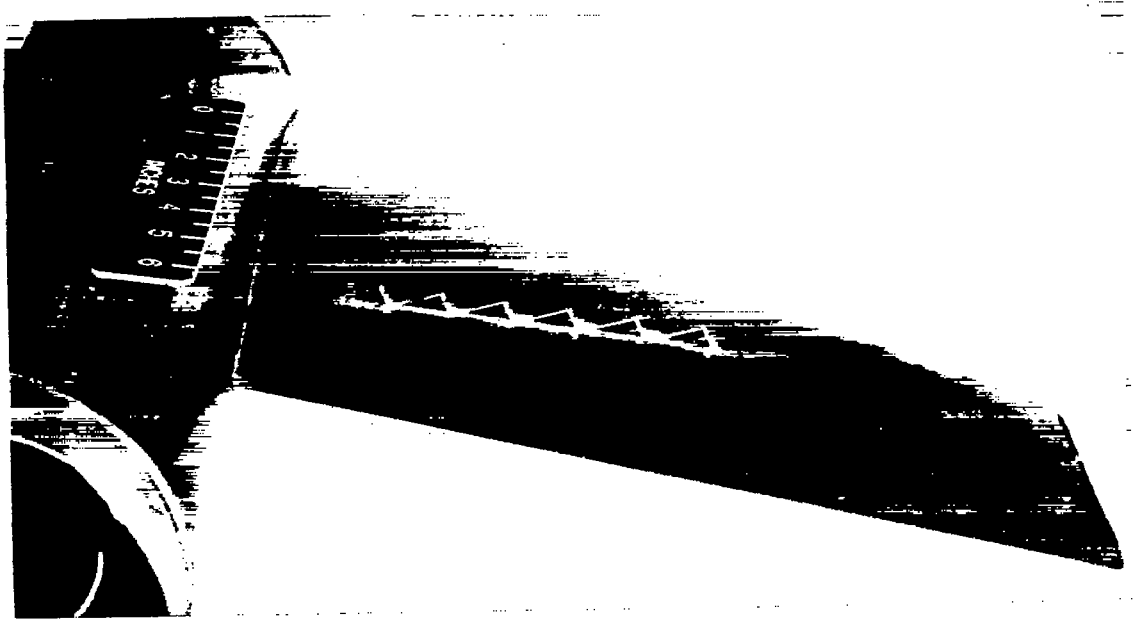

L-76027

(b) 20° spoiler.

Figure 4.- Photographs of wing-spoiler combinations.

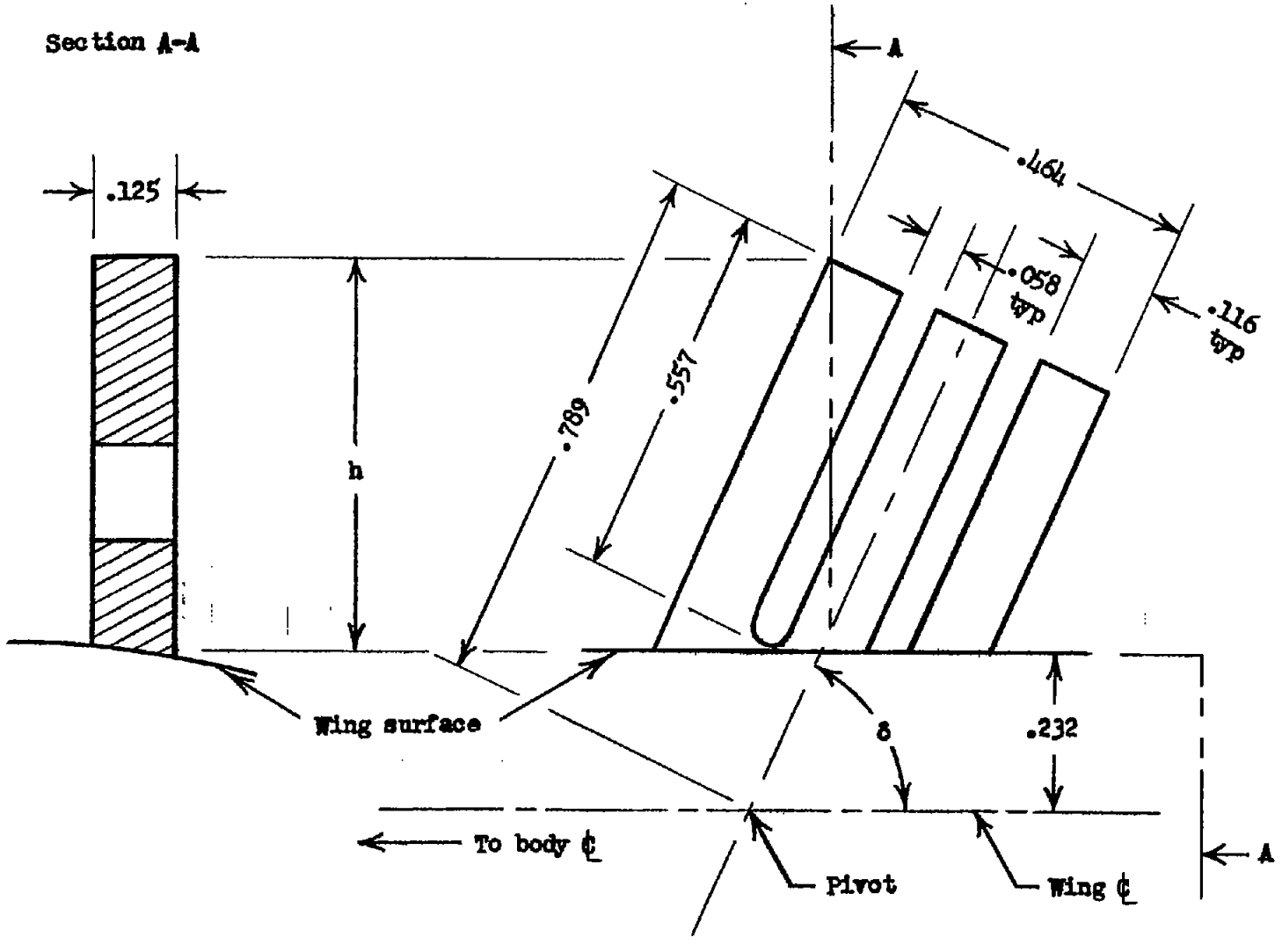

Figure 5.- Spoiler geometry. All dimensions are in inches.

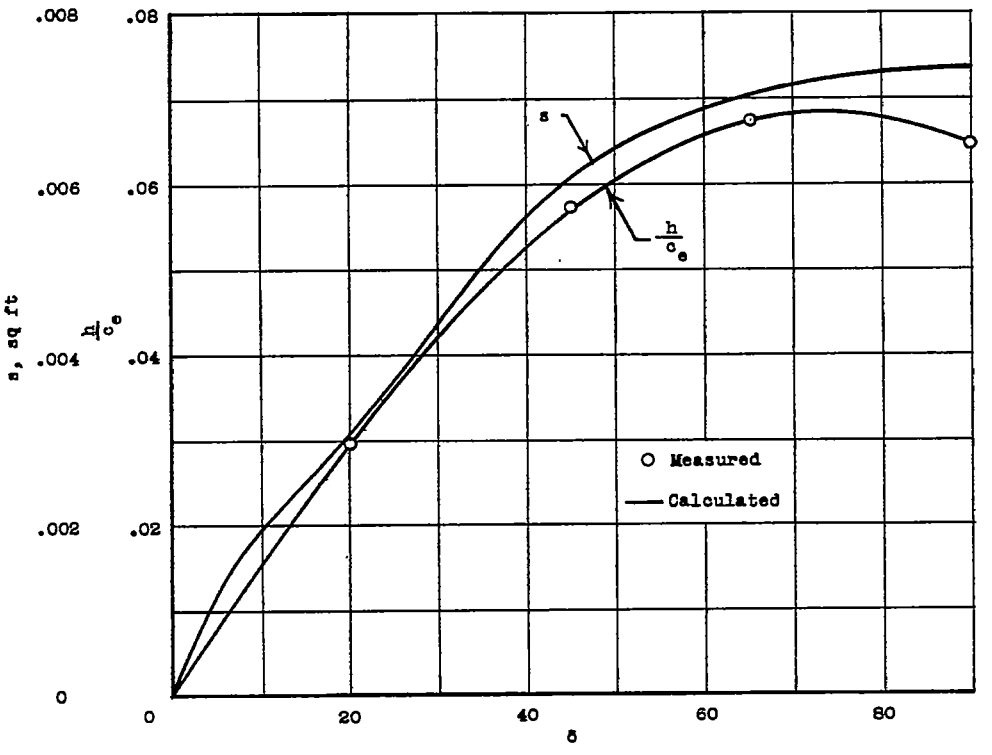

Figure 6.- Variation of peak spoiler height in percent chord and total spoiler frontal area with spoiler deflection.

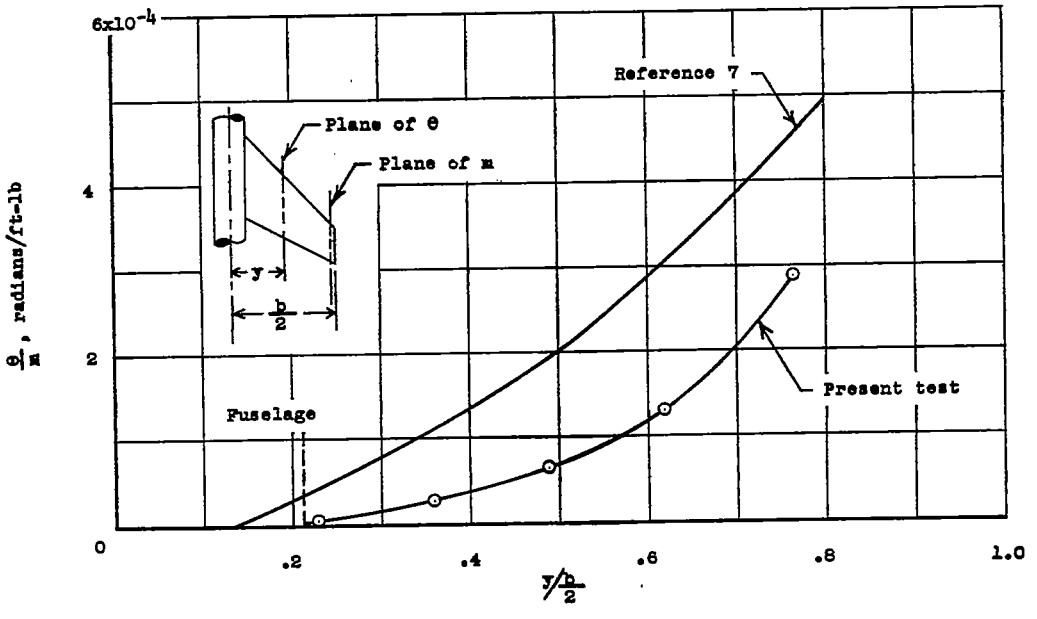

Figure 7.- Rate of change of wing torsional flexibility parameter with wing [redacted]

[redacted]

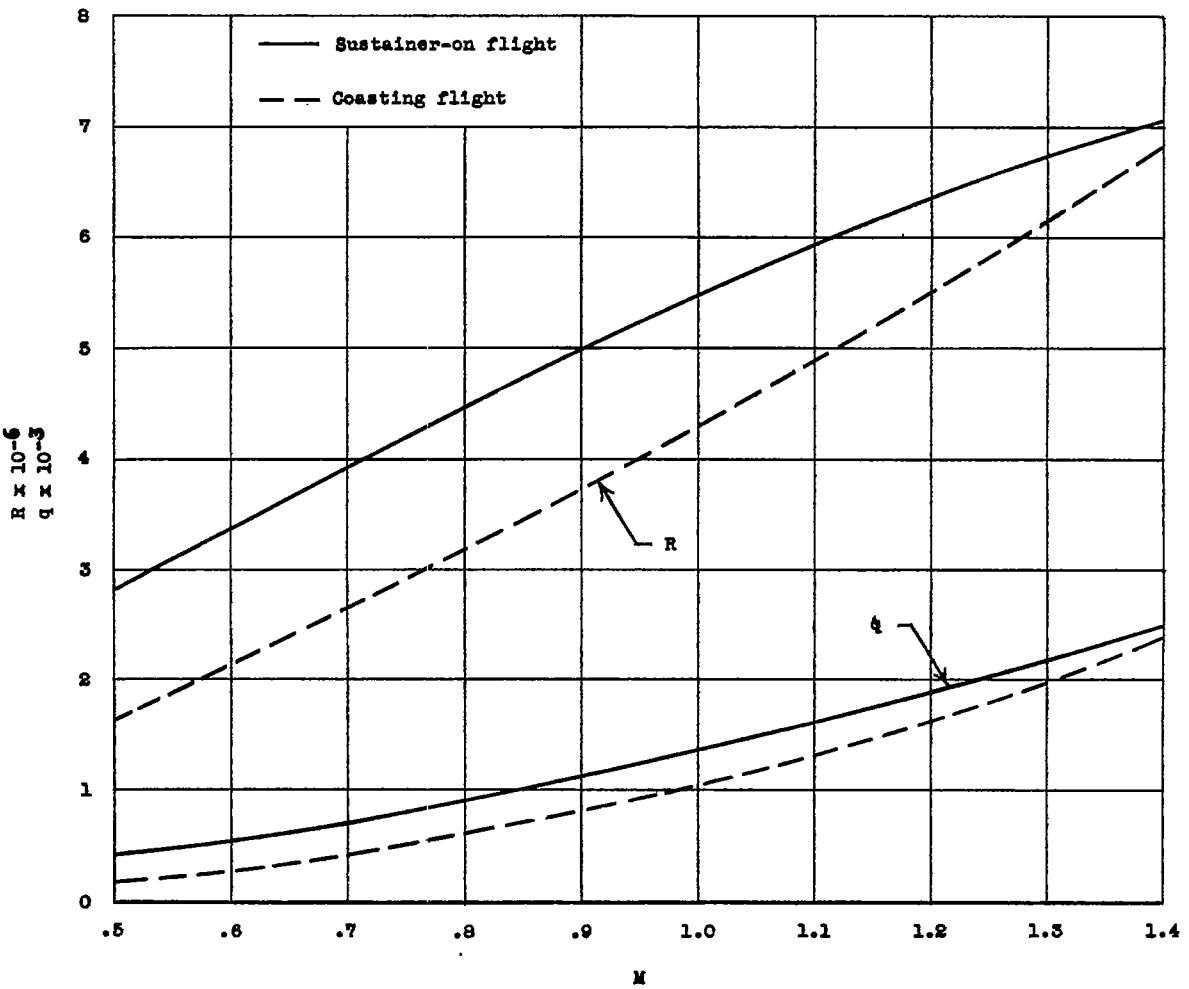

Figure 8.- Typical variation of Reynolds number and dynamic pressure with Mach number.

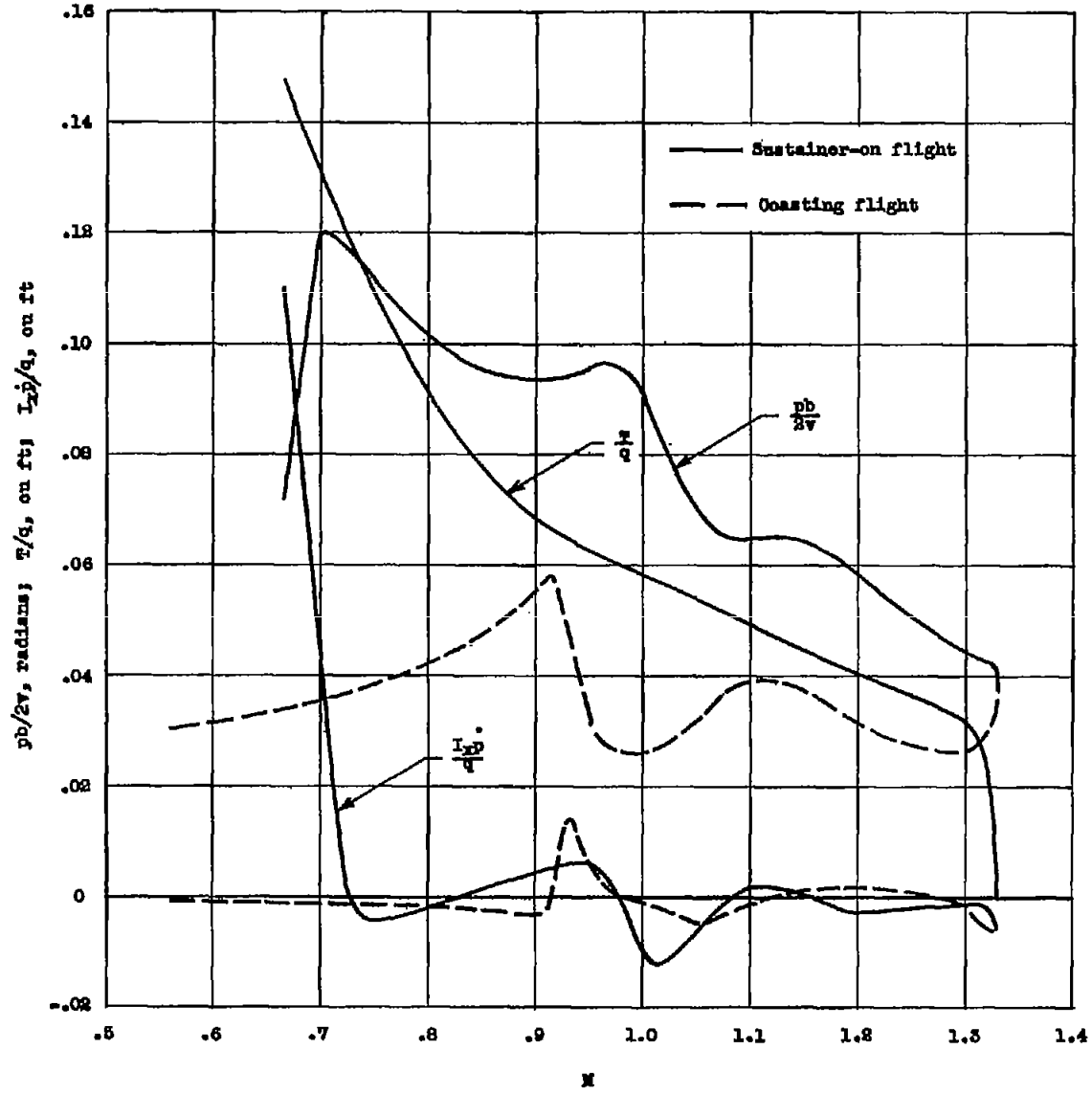

Figure 9.- Typical variation of test parameters with Mach number, $\delta = 65^{\circ}$.

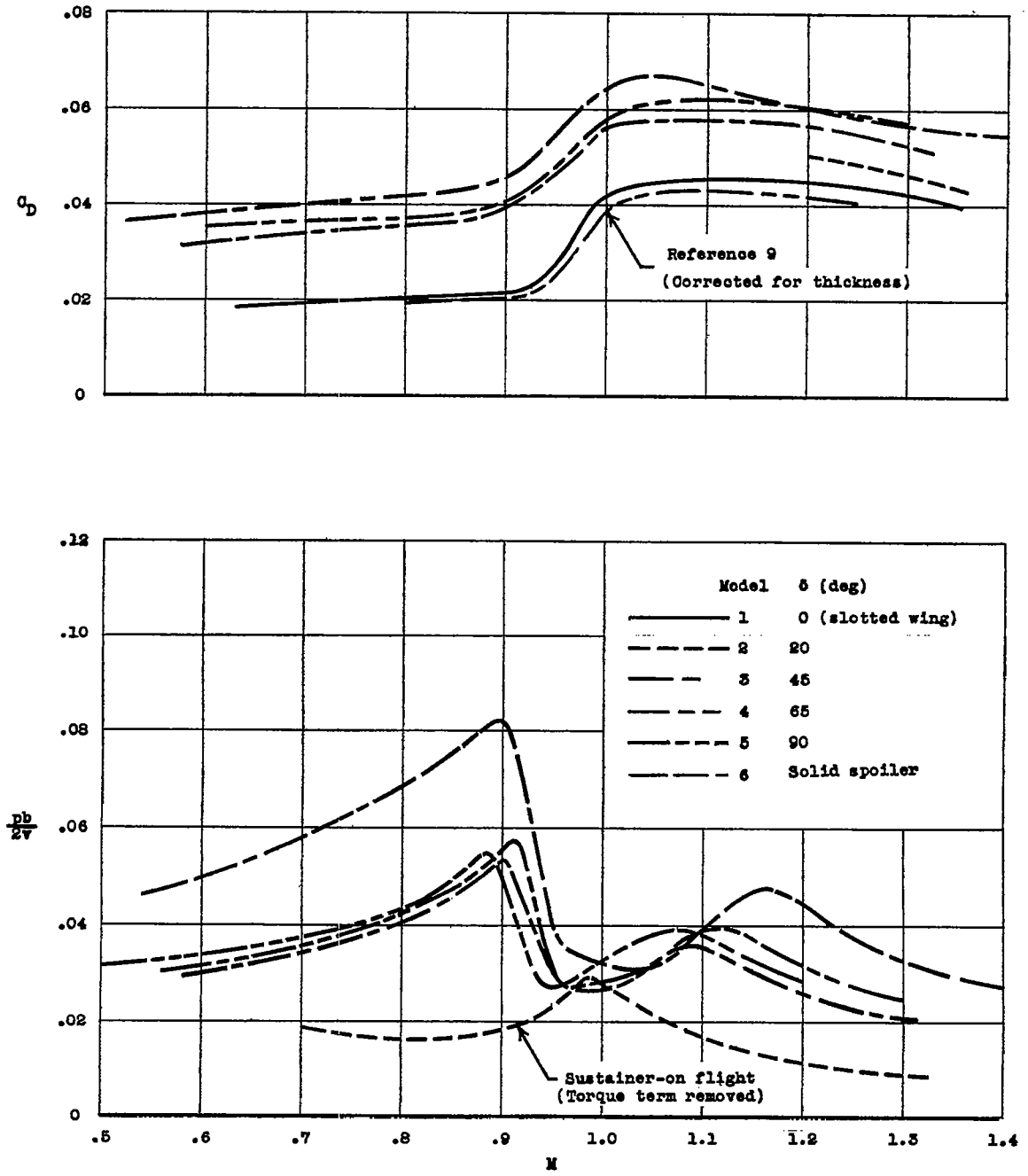

Figure 10.- Variation of total drag coefficient and rolling effectiveness with Mach number for various spoiler deflections. Coasting flight.

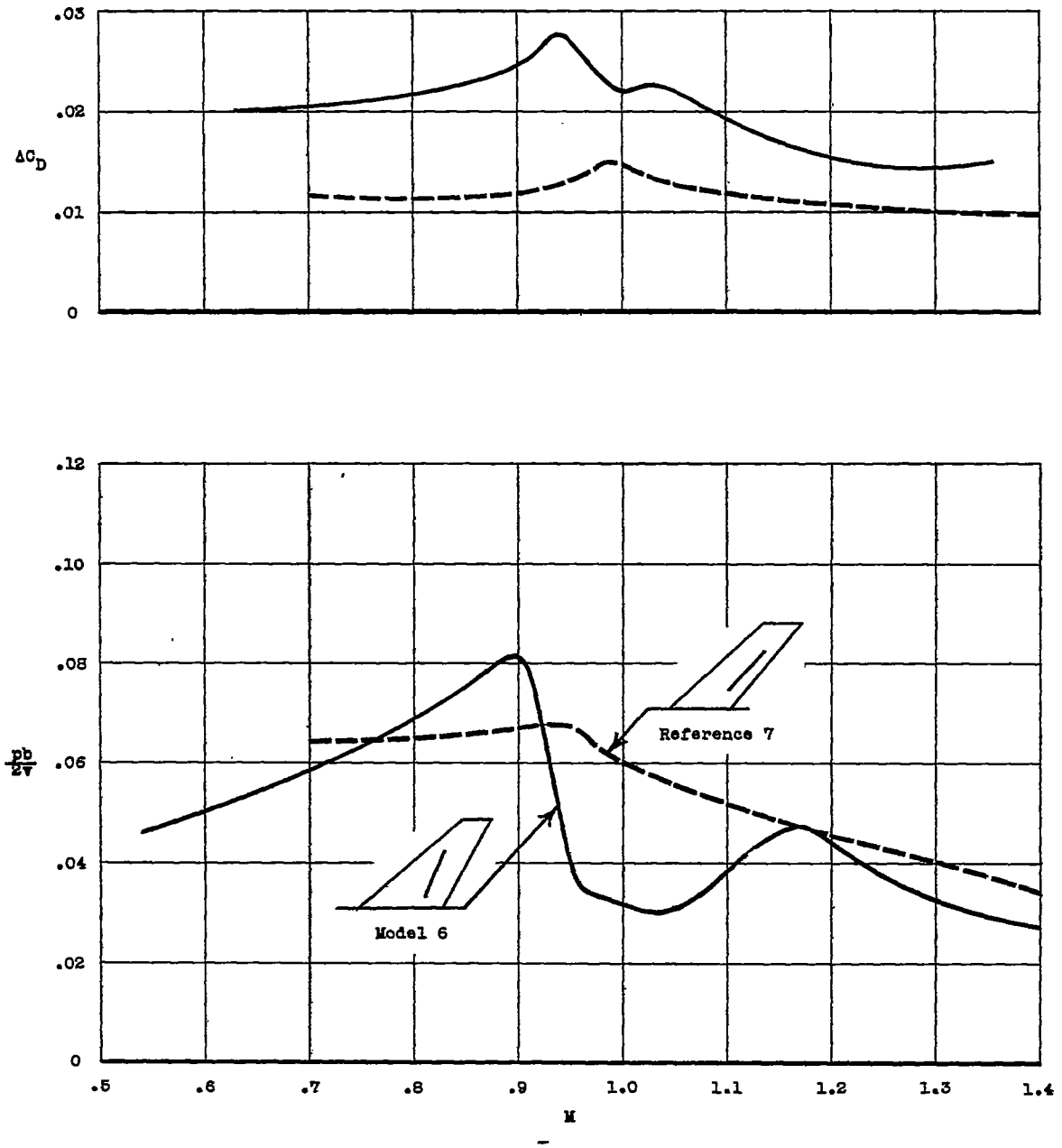

Figure 11.- Comparison of variation of incremental drag coefficient and rolling effectiveness with Mach number for solid spoilers of present test and reference 7.

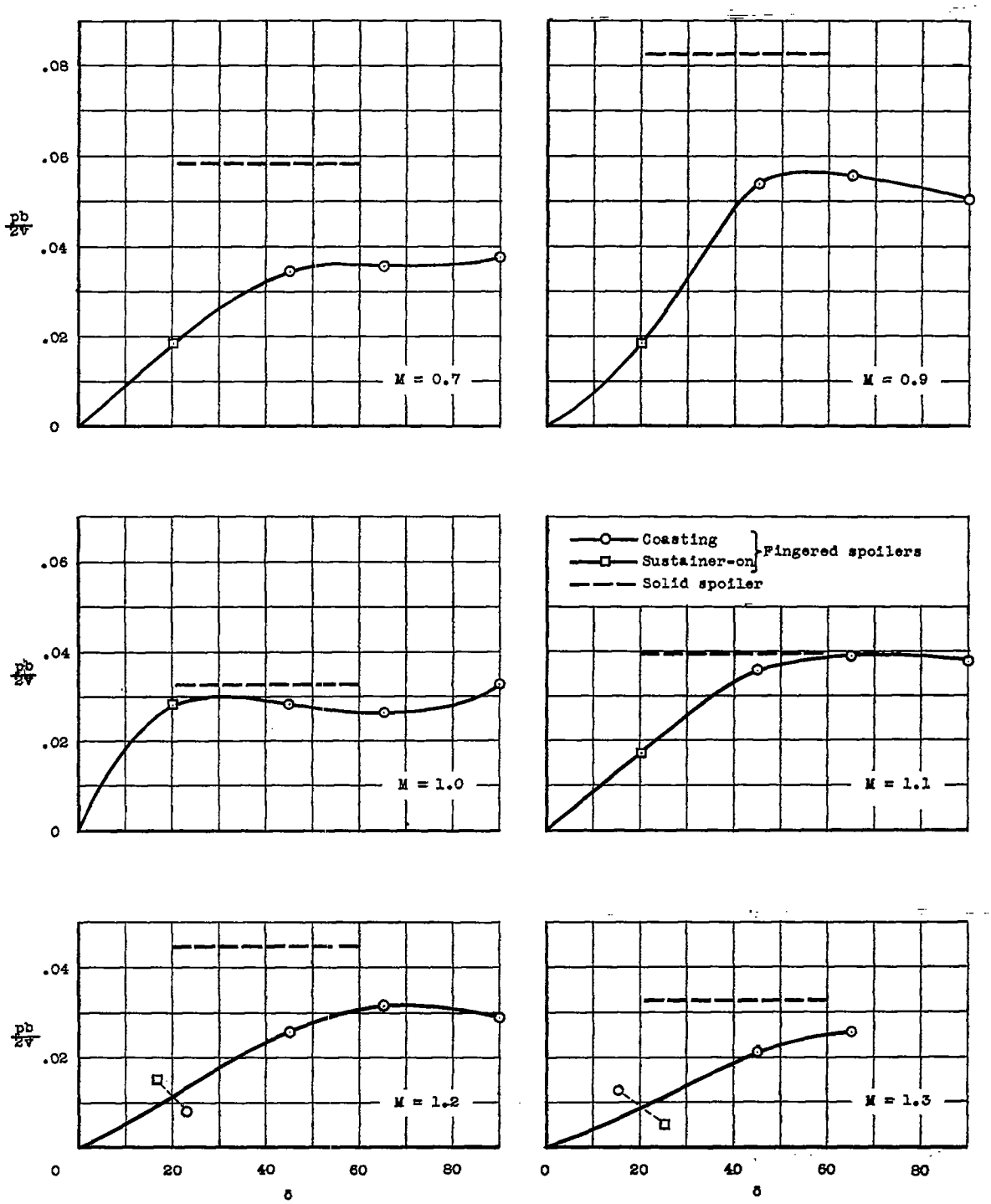

Figure 12.- Rolling effectiveness as a function of spoiler deflection at six Mach numbers.

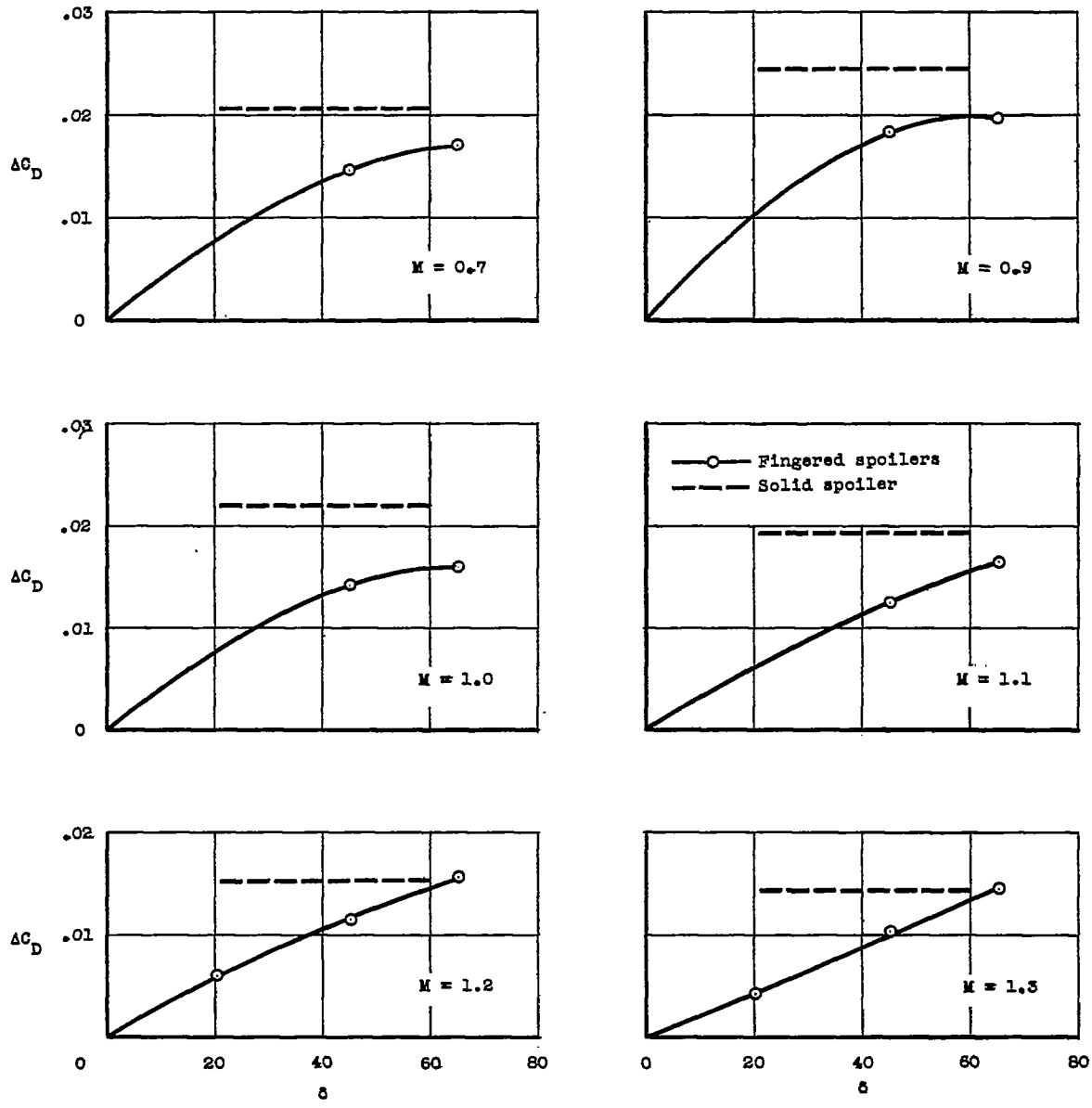

Figure 13.- Incremental spoiler drag coefficient based on model 1 as a function of spoiler deflection at six Mach numbers.

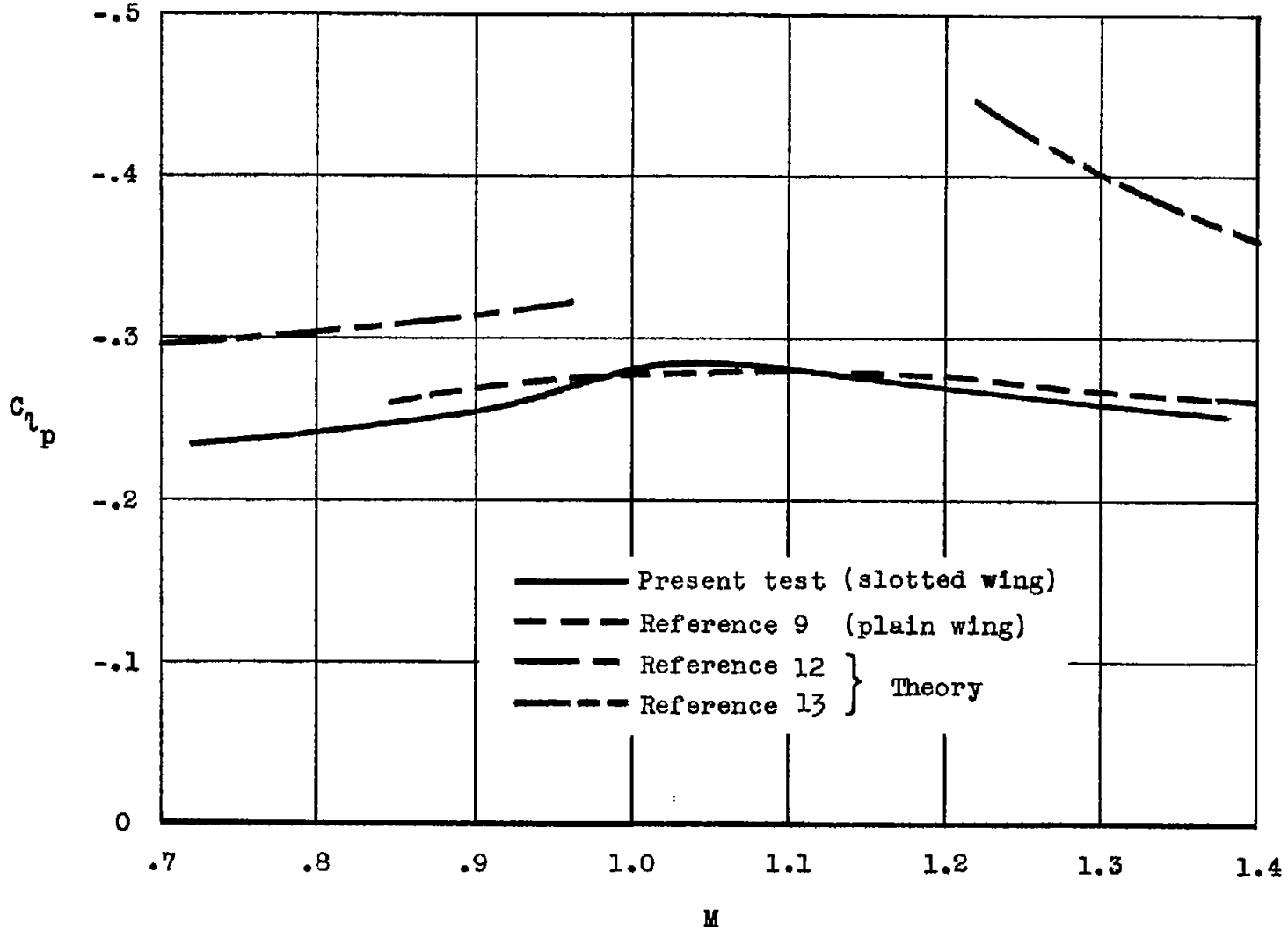

Figure 14.- Variation of wing damping-in-roll coefficient with Mach number for zero spoiler deflection.

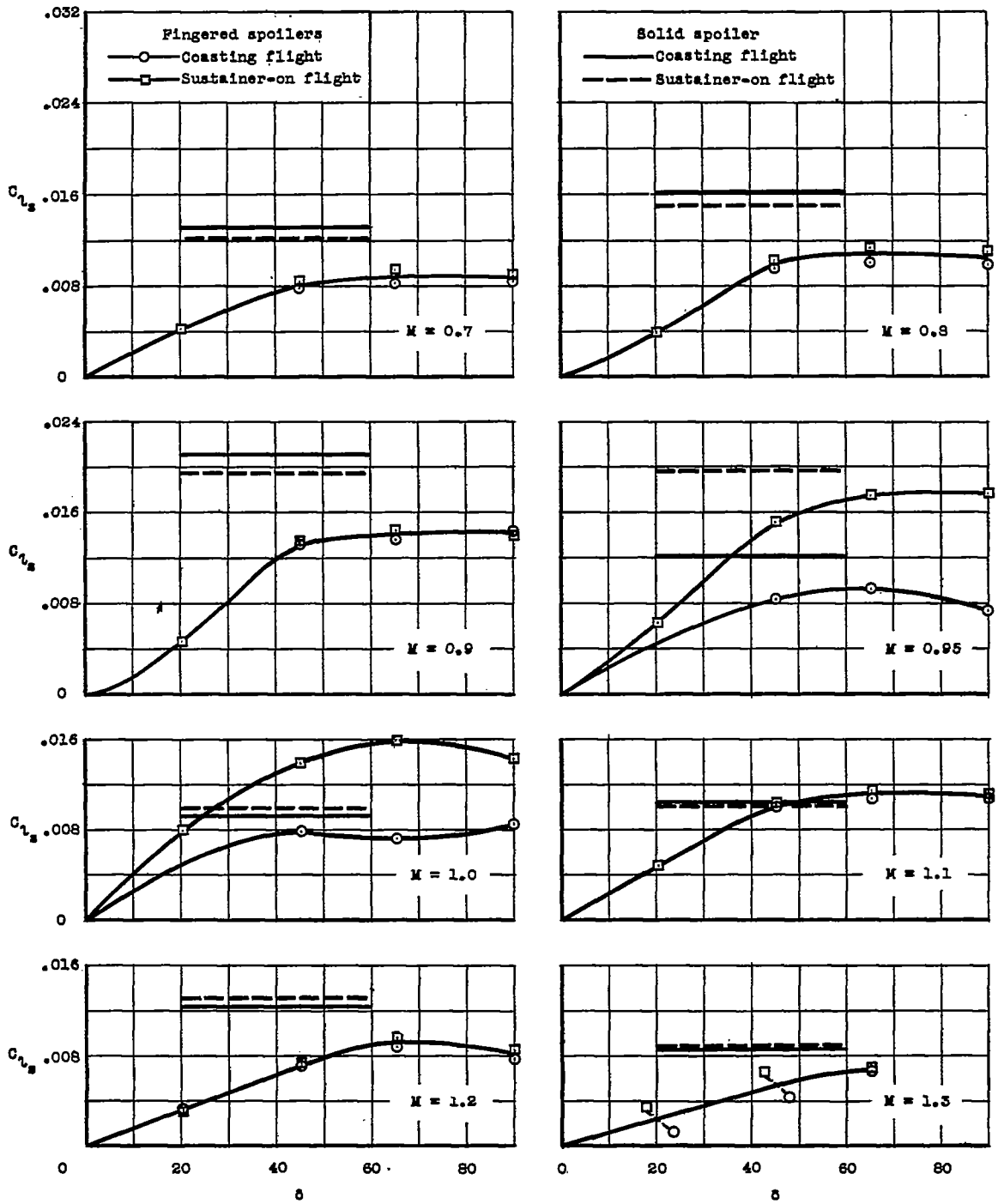

Figure 15.- Spoiler rolling-moment coefficient as a function of spoiler deflection at eight Mach numbers.

NACA-Langley - 1-14-54 - 325